PREDICTION OF THE TEMPERATURE OF A DRILL IN DRILLING LUNAR ROCK SIMULANT IN A VACUUM

by

Jinsheng CUI, Xuyan HOU*, Zongquan DENG, Wanjing PAN, and Qiquan QUAN

Department of Mechatronics Engineering, Harbin Institute of Technology, Harbin, China

Original scientific paper
https://doi.org/10.2298/TSCI141023051C

In this article, the temperature of a sampling drill in drilling lunar rock simulant in a high-vacuum environment was studied. The thermal problem was viewed as a 1-D transient heat transfer problem in a semi-infinite object. The simplified drill was modeled using heat conduction differential equation and a fast numerical calculation method is proposed on this basis, with time and the drill discretized. The model was modified to consider the effects of radiation, drill bit configuration, and non-constant heat source. A thermal analysis was conducted using ANSYS Workbench to determine the value of the equivalent correction coefficient proposed in this paper. Using fiber Bragg grating temperature measurement method, drilling experiments were conducted in a vacuum, and the results were compared to the model. The agreement between model and experiment was very good.

Key words: *drill temperature, vacuum, radiation, fast numerical calculation*

Introduction

According to Chinese lunar exploration project planning, the sampling device carried by the detector will collect lunar sample. After a comparison and analysis of alternatives, sampling by drilling was judged to be a feasible approach. Given the dry drilling process, the high-vacuum environment of the lunar surface, and the poor thermal properties of lunar soil [1, 2], it is reasonable to expect that the drill bit may reach a very high temperature, which could result in structural damage to the drill bit. For reasons of reliability and restricted internal space, temperature sensors cannot be installed in the drill for monitoring or online control purposes. In addition, the existence of lunar rocks and the uncertainty associated with the physical properties of lunar soil and rocks make it difficult to estimate the torque and force that will act on the drill, both of which are important to prediction of the temperature of the drill.

Research on drilling temperatures has been focused in the field of metal cutting. Devries *et al.* [3] modeled the drill as a half-infinite object, and modeled the cutting forces and heat generation of the drill bit to calculate the temperatures along the cutting edges. However, the model results did not agree with their experiments. Saxena *et al.* [4] and Watanabe *et al.* [5] calculated the temperatures along the cutting edges of a drill using the finite difference method and the finite element method. Their results were similar to those of Devries. After making some improvements to the previous model, Agapiou *et al.* [6] and Agapiou and Stephenson [7] developed an analytical model to predict the temperature of a twist drill on the flank face and

* Corresponding author, e-mail: houxuyan@hit.edu.cn

cutting edge, and explain thermal phenomena during the cutting process. The knowledge about the torque was found to be necessary for calculating the temperatures. Fuh *et al.* [8] also improved their method, and calculated the temperature distribution of a drill using 3-D finite element method. In their study, the effects of cutting depth, cutting speed, web thickness, and helix angle on the temperature were investigated. Bono and Ni [9, 10] developed a drill-foil thermocouple system for measuring the temperature distribution along the cutting edges. Their experiments showed that the maximum temperature occurs near the chisel edge. Their calculated results obtained by taking both friction and cutting into consideration, were consistent with their experimental results. Li and Shih [11] studied the thrust force, torque, and temperature observed during titanium drilling. The tool temperature distribution was developed based on oblique cutting in an elementary cutting tool by using Abaqus, and measured using thermocouples embedded on the drill flank face. Wu and Han [12] predicted the maximum temperature in dry drilling using finite element model. The effect of drilling velocities and feed rates on the temperature were investigated. The comparison between experimental tests by an infrared camera and simulation was carried out. The results indicated that the errors are less than 15%. De Sousa *et al.* [13] presented an inverse technique for estimating the temperature and heat flux at the tool-piece interface during drilling.

To determine the temperature distribution along cut edges, thermal models usually focus on the complex local region of cut edges, which makes the solution complicated and requires long computation times. In addition, because of air convection and other auxiliary heat dissipation, the current models scarcely consider radiation, which obviously cannot be ignored in the case of a high-vacuum environment such as the lunar environment. The need to consider radiation is rarely mentioned in the literature to date on temperature fields in mechanical rock drilling. The aims of this work were to investigate a thermal model for this situation, in which high temperatures can easily be produced, and to develop a method to predict the temperature of the drill. For the purpose of rapid online monitoring in the future, the algorithm must be as simple as possible to minimize the computation time while achieving sufficient accuracy. The method should also be adaptable to various drill bit configurations. In this study, the results obtained using the algorithm and the results of experiments were compared. The effect of radiation on the temperature field was examined.

Fundamentals

Consider a hollow drill and a lunar rock simulant, as shown in fig. 1, in a vacuum with an initial temperature of T_0. Heat is generated at the interface between the drill and the lunar rock simulant because of friction and cutting. The heat is mostly conducted in the direction of the drill and radiated outward into the environment. The portion of the heat conducted into the rock and the temperature of the rock are not discussed in this paper. It is assumed that the temperature of the environment does not change.

If most of the drill is embedded in the lunar rock simulant, the radiation of heat from the drill will be different from that considered in this study. However, given the limits of the current capabilities with respect to drilling on the Moon, deep drilling into lunar rock is not feasible at present. In this study, only shallow drilling was examined.

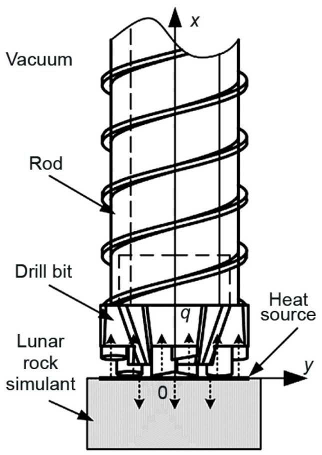

Figure 1. Thermal model

Model for 1-D heat conduction in a semi-infinite rod

Only a long hollow rod was initially considered as a semi-infinite objective, regardless of the bit and thread. Changes in the material's thermophysical properties with temperature were ignored, and it was assumed that the temperatures of all cross-sections were the same. This then becomes a problem of transient heat conduction in a 1-D, semi-infinite material with constant thermophysical properties and without inner heat sources. The heat conduction equation is expressed:

$$\frac{\partial T}{\partial \tau} = a \frac{\partial^2 T}{\partial x^2} \tag{1}$$

The analytical solution of eq. (1) is:

$$T(\tau, x) = \frac{C_0}{2\sqrt{\pi a \tau}} \exp\left(-\frac{x^2}{4a\tau} \right) \tag{2}$$

The boundary condition for the problem is the point heat source at the front of the drill (where $x = 0$). If the heat source is a transient point heat source with energy Q, an energy balance applied to the semi-infinite rod would be expressed:

$$\frac{Q}{\rho c} = \int_0^\infty AT\mathrm{d}x = \int_0^\infty \frac{AC_0}{2\sqrt{\pi a \tau}} \exp\left(-\frac{x^2}{4a\tau} \right) \mathrm{d}x = AC_0 \int_0^\infty \frac{1}{2\sqrt{\pi}} \exp\left(-\frac{1}{2}\frac{x^2}{2a\tau} \right) \mathrm{d}\left(\frac{x}{\sqrt{2a\tau}} \right) = \frac{AC_0}{2} \tag{3}$$

Considering heat conduction only, the temperature in the semi-infinite rod caused by a transient point heat source with energy, Q, is given:

$$T_t(\tau, x) = \frac{Q}{A\rho c\sqrt{\pi a \tau}} \exp\left(-\frac{x^2}{4a\tau} \right) \tag{4}$$

If the heat source is continuous, with a rate of heat generation, q, it can be considered as a transient point heat source during each infinitesimal time increment $\mathrm{d}\tau$. The temperature in the rod at time τ_0 caused by the continuous point heat source can be seen as the sum of the temperatures caused by the heat sources in all of the infinitesimal time increments before τ_0.The analytical expression for this is:

$$T_{ca}(\tau_0, x) = \int_0^{\tau_0} \frac{q}{A\rho c\sqrt{\pi a \tau}} \exp\left(-\frac{x^2}{4a\tau} \right) \mathrm{d}\tau \tag{5}$$

Note that the variable τ in eq. (5) accounts for the time between infinitesimal time increment $\mathrm{d}\tau$ and τ_0 rather than the time from 0 to $\mathrm{d}\tau$.

Thus, if only heat conduction due to the continuous point heat source in the front of the drill is considered, the temperature in the semi-infinite rod at time τ_0 is given by:

$$T(\tau_0, x) = T_{ca}(\tau_0, x) + T_0 \tag{6}$$

Impact of radiation on the temperature

When radiation is considered, the temperature in the drill can be seen as the sum of the heat conduction due to the heat source at the front of the drill and the radiation of heat from the drill into the environment. In this study, the impact of radiation on the temperature was divided into two parts. The first part was the temperature reduction caused directly by the heat loss due to radiation, referred to hereinafter as radiation heat loss. The other part

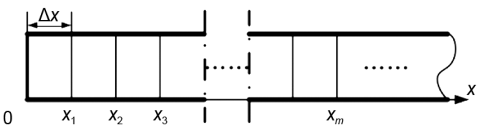

Figure 2. Discretization of the drill

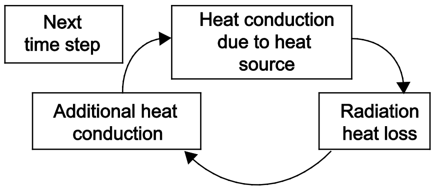

Figure 3. Temperature calculation procedure considering radiation

was heat conduction due to the difference in temperature reduction along the drill in the first part, referred to hereinafter as additional heat conduction.

Radiation and conduction are usually coupled because radiation is related to the current temperature. To decouple them, time needs to be discretized into time steps of $\Delta\tau$. The drill also needs to be discretized into small elements with length Δx, as shown in fig. 2, to calculate the additional heat conduction. The temperature can be predicted to decrease gradually along the drill, and the temperature far from the head is usually not of concern. Therefore, calculating the temperature for a certain number m of elements at the front of the drill can ensure sufficient accuracy and reduce the computation time. Then, the temperature of the drill can be calculated according to the procedure illustrated in fig. 3.

After time discretization, the heat conduction due to the heat source at the front of the drill needs to be modified. According to eq. (5), at the end of the first time step, the temperature caused by the heat source during the first time step can be written:

$$T_{c1j} = \int_0^{\Delta\tau} \frac{q}{A\rho c\sqrt{\pi a\tau}} \exp\left(-\frac{x^2}{4a\tau}\right) d\tau \tag{7}$$

At the end of the second time step, T_{c1j} becomes:

$$T_{c2j} = \int_{\Delta\tau}^{2\Delta\tau} \frac{q}{A\rho c\sqrt{\pi a\tau}} \exp\left(-\frac{x^2}{4a\tau}\right) d\tau \tag{8}$$

Meanwhile, the temperature caused by the heat source during the second time step is still T_{c1j}. Therefore, at the end of the second time step, the temperature caused by the heat source is:

$$T_{cs2j} = T_{c1j} + T_{c2j} = T_{ca}(2\Delta\tau, x_j) \tag{9}$$

Similarly,

$$T_{cij} = \int_{(i-1)\Delta\tau}^{i\Delta\tau} \frac{q}{A\rho c\sqrt{\pi a\tau}} \exp\left(-\frac{x^2}{4a\tau}\right) d\tau \tag{10}$$

At the end of any time step, $i\Delta\tau$, the temperature caused by the heat source is:

$$T_{csij} = T_{c1j} + T_{c2j} + \ldots + T_{cij} = T_{ca}(\mathrm{i}\Delta\tau, x_j) \tag{11}$$

Note that T_{cij} and eq. (11) make sense only in the case that the heat source at the front of the drill is constant. The case of a non-constant heat source is discussed in the section *Non-constant heat source*.

The temperature reduction of a drill element during any time step as a direct loss of heat due to radiation can be determined from the Stefan-Boltzmann law. However, with the increase of drilling depth, part of the drill will enters into the lunar rock simulant. The temperature reduction of the submerged portion is complex. The radiation remains and consists of two parts. One part is multiple radiation between the drill and the lunar rock simulant, and the other part is radiation to the environment (because the diameter of drilled hole is usually greater than diameter of the drill). The temperature reduction caused by radiation of the submerged drill elements can be predicted as a function of the temperature field of drill and lunar rock simulant, and will be much less. To simplify the model, the radiation of a submerged drill element is ignored once the drill element is totally submerged. That is:

$$\begin{cases} T_{\mathrm{r}ij} = \dfrac{\varepsilon\sigma\Delta\tau}{c\rho d_j}[(T'_{ij}+273.15)^4-(T_0+273.15)^4] & (h < j\Delta x) \\ T_{\mathrm{r}ij} = 0 & (h \geq j\Delta x) \end{cases} \tag{12}$$

where

$$T'_{ij} = T_{i-1,j} + T_{\mathrm{c}ij} \tag{13}$$

where T'_{ij} is the temperature of the drill element at time $i\Delta\tau$, and position x_j without consideration of radiation during the current time step. However, eq. (13), related to T_{cij}, is also not valid in the case of a non-constant heat source. Equation (13) is replaced by a more universal equation later.

Additional heat conduction can be calculated using the Taylor expansion method. The time step is divided into smaller time elements, that is $\Delta^2\tau = \Delta\tau/n_2$. Because the heat source at the front of the drill does not need to be considered here and additional heat conduction after x_m is ignored, the boundary conditions of both sides are heat insulation. Additional heat conduction can be calculated iteratively by:

$$\begin{cases} T_{\mathrm{r}i1}^{(k)} = T_{\mathrm{r}i1}^{(k)} - \dfrac{\left[T_{\mathrm{r}i1}^{(k-1)} - T_{\mathrm{r}i2}^{(k-1)}\right]a\Delta^2\tau}{\Delta x^2} & \\ T_{\mathrm{r}ij}^{(k)} = T_{\mathrm{r}ij}^{(k-1)} - \dfrac{\left[2T_{\mathrm{r}ij}^{(k-1)} - T_{\mathrm{r}i,j-1}^{(k-1)} - T_{\mathrm{r}i,j+1}^{(k-1)}\right]a\Delta^2\tau}{\Delta x^2} & j = 2, 3, \cdots, m-1 \quad k = 1, 2, \cdots, n_2 \\ T_{\mathrm{r}im}^{(k)} = T_{\mathrm{r}im}^{(k)} - \dfrac{\left[T_{\mathrm{r}im}^{(k-1)} - T_{\mathrm{r}i,m-1}^{(k-1)}\right]a\Delta^2\tau}{\Delta x^2} & \end{cases} \tag{14a}$$

After iterative calculation, $T_{\mathrm{r}ij}$ becomes $T'_{\mathrm{r}ij}$. The iterative calculation is denoted by function H:

$$T'_{\mathrm{r}ij} = H(T_{\mathrm{r}ij}) \tag{14b}$$

Because the additional heat conduction for $T_{\mathrm{r}ij}$ of every time step needs to be calculated not only for the current time step but also for all of the rest, additional heat conduction for all time steps can be calculated from:

$$\begin{cases} T_{\mathrm{rs}1j} = T_{\mathrm{r}1j}, \quad T_{\mathrm{rs}2j} = T'_{\mathrm{rs}1j} + T_{\mathrm{r}2j}, \cdots\cdots, T_{\mathrm{rs}ij} = T'_{\mathrm{rs}i-1,j} + T_{\mathrm{r}ij} \\ T'_{\mathrm{rs}ij} = H(T_{\mathrm{rs}ij}) \end{cases} \quad i = 2, 3, \cdots, n \tag{15}$$

The temperature of the drill during the current time step is then expressed:

$$T_{ij} = T_0 + T_{csij} - T'_{rsij} = T_0 + T(i\Delta\tau,\, x_j) - T'_{rsij} \tag{16}$$

Equation (13) can become a more universal form:

$$T'_{ij} = T_0 + T_{csij} - T_{rsi-1,\, j} = T_0 + T(i\Delta\tau,\, x_j) - T_{rsi-1,\, j} \tag{17}$$

Impact of drill bit configuration on the temperature

To simplify the analysis, drill bit was ignored in the preceding discussion. In reality, the configuration of the drill bit has an influence on the temperature. Consider a drill bit with cross-sectional area $A_b(x)$. The drill bit is divided into non-uniform parts, each of which is deemed to have the same cross-sectional area, as shown in fig. 4.

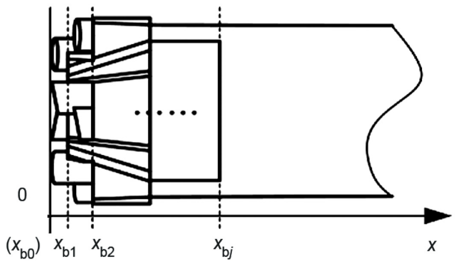

Figure 4. Bit configuration

The number of parts, denoted by l, is determined on the basis of the complexity of the drill bit, such that, for a given bit configuration, the cross-sectional areas of these parts are constant values. Thus, $A_b(x)$ can be piecewise represented as a proportion of the cross-sectional area of the rod:

$$A_b(x) = k_{Aj}A, \qquad x_{bj-1} < x < x_{bj}, \qquad j = 1, 2, \cdots, l \tag{18}$$

Assuming as before that the temperatures of all cross sections are the same, eq. (3) becomes:

$$\frac{Q}{\rho c} = \sum_{j=1}^{l} \int_{x_{bj-1}}^{x_{bj}} (k_{Aj} - 1) A T(x) \mathrm{d}x + \int_0^{\infty} A T(x) \mathrm{d}x =$$

$$= AC_0 \sum_{j=1}^{l} (k_{Aj} - 1) \int_{x_{bj-1}}^{x_{bj}} \frac{1}{\sqrt{2\pi}} \exp\left(-\frac{1}{2} \frac{x^2}{2a\tau} \right) \mathrm{d}\left(\frac{x}{\sqrt{2a\tau}} \right) + \frac{AC_0}{2} \tag{19a}$$

With the changes of variables, $s = x/\sqrt{2a\tau}$ and $s_j = x_{bj}/\sqrt{2a\tau}$, eq. (19a) becomes:

$$\frac{Q}{\rho c} = AC_0 \sum_{j=1}^{l} (k_{Aj} - 1) \int_{s_{j-1}}^{s_j} \frac{1}{\sqrt{2\pi}} \exp\left(-\frac{s^2}{2} \right) \mathrm{d}s + \frac{AC_0}{2} = \left(k_b + \frac{1}{2} \right) AC_0 \tag{19b}$$

where

$$k_b = \sum_{j=1}^{l} (k_{Aj} - 1) \int_{s_{j-1}}^{s_j} \frac{1}{\sqrt{2\pi}} \exp\left(-\frac{s^2}{2} \right) \mathrm{d}s \tag{20}$$

is a function of configuration of the drill bit, thermophysical properties of the material, and time. The integral term is a normal distribution, which can be obtained easily. For given bit configuration and material, k_b is a function only of time. The value of k_b for an individual time step is denoted by k_{bi}, given by:

$$k_{\mathrm{b}i} = k_{\mathrm{b}}\Big|_{\tau=\frac{2i-1}{2}\Delta\tau} \tag{21}$$

The value of $k_{\mathrm{b}i}$ can be calculated for a given time step.

Thus, considering the impact of the drill bit configuration on the temperature, eq. (4) and eq. (10), respectively, become:

$$T_{\mathrm{t}}(\tau, x) = \frac{q\,\mathrm{d}\tau}{(2k_{\mathrm{b}i}+1)A\rho c\sqrt{\pi a\tau}} \exp\left(-\frac{x^2}{4a\tau}\right) \tag{22}$$

$$T_{\mathrm{c}ij} = \int_{(i-1)\Delta\tau}^{i\Delta\tau} \frac{q}{(2k_{\mathrm{b}i}+1)A\rho c\sqrt{\pi a\tau}} \exp\left(-\frac{x^2}{4a\tau}\right) \mathrm{d}\tau \tag{23}$$

In addition, the thickness of the drill in eq. (12), d_j, is not a constant anymore. The equivalent thickness of the corresponding drill element in fig. 2 is $d_j = V_j/2\pi r\Delta x$. Here V_j is the volume of the corresponding drill element.

This modified method is obviously applicable to any drill bit configuration.

Non-constant heat source

To simplify the analysis, the heat source at the front of the drill was deemed to be constant in the preceding discussion. However, this heat source is usually not constant. A non-constant heat source can be discretized according to time steps, and can be expressed:

$$q(\tau) = q_i = k_e M_i n_{\mathrm{roti}} \quad (i-1)\Delta\tau < \tau < i\Delta\tau \tag{24}$$

where M_i and $n_{\mathrm{r}i}$ are the average torque and rotational speed, respectively, during the corresponding time step. The k_e term is a correction coefficient, the value of which needs to be determined by comparing finite element simulation results to experimental results, as discussed in the section *Determination of correction coefficient*.

At the end of any time step $i\Delta\tau$, the temperature of the drill caused by the heat source $q_k(1 \le k \le i)$ can be written:

$$T_{\mathrm{c}kj}^{(i)} = \int_{(i-k)\Delta\tau}^{(i-k+1)\Delta\tau} \frac{q_k}{[2k_{\mathrm{b}(i-k+1)}+1]A\rho c\sqrt{\pi a\tau}} \exp\left(-\frac{x_j^2}{4a\tau}\right) \mathrm{d}\tau \tag{25}$$

At the end of $i\Delta\tau$, the temperature caused by the heat source is redefined:

$$\begin{aligned} T_{\mathrm{cs}ij} &= \sum_{k=1}^{i} T_{\mathrm{c}kj}^{(i)} = \sum_{k=1}^{i} \frac{q_k}{2k_{\mathrm{b}(i-k+1)}+1} \int_{(i-k)\Delta\tau}^{(i-k+1)\Delta\tau} \frac{1}{A\rho c\sqrt{\pi a\tau}} \exp\left(-\frac{x_j^2}{4a\tau}\right) \mathrm{d}\tau = \\ &= \sum_{k=1}^{i} \frac{q_k}{2k_{\mathrm{b}(i-k+1)}+1} I_{i-k+1,j} \end{aligned} \tag{26}$$

where

$$I_{ij} = \int_{(i-1)\Delta\tau}^{i\Delta\tau} \frac{1}{A\rho c\sqrt{\pi a\tau}} \exp\left(-\frac{x_j^2}{4a\tau}\right) \mathrm{d}\tau \tag{27}$$

Equation (26) replaces eq. (11) in the case of a non-constant heat source at the front of the drill.

Calculating eq. (26) can be expected to involve a long computation time because of the integral. However, when the bit configuration, bit material, time step, and drill elements are all selected, the integral is easily solved. Its value can be calculated in advance and treated as a constant in the temperature calculation, which reduces the computation time dramatically.

In conclusion, the temperature of the drill in a lunar rock simulant in a vacuum can be calculated according to the process shown in fig. 5.

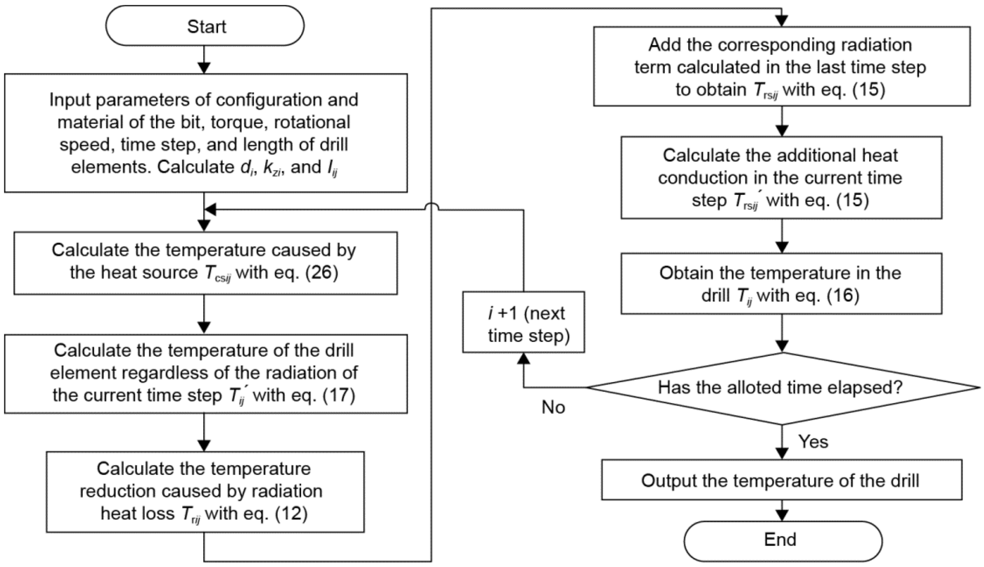

Figure 5. Calculation process for the temperature of a drill in a lunar rock simulant in a vacuum

It can be seen from fig. 5 that on the basis of the previous numerical calculation method, we can obtain the temperature of any position (corresponding to time step $i\Delta\tau$) alone the drill at any time (corresponding to drill element x_j) as long as we know necessary parameters, such as torque, rotational speed in drilling process, and correction coefficient k_e introduced in eq. (24). In the next sections, we conducted drilling experiments in a vacuum, controlling the rotational speed and monitoring the torque and temperature, to obtain correction coefficient k_e and verify the method.

Experimental apparatus

There are methods to measure cutting temperature based on thermocouple or radiation [14]. However, during high-speed drilling in a vacuum, given the poor thermal conductivity of the drilling objects, the temperature of the bit cannot be measured directly by conventional methods. Therefore, the fiber Bragg grating (FBG) temperature measurement method [15] was used in the experiments. Drilling temperature measurement testbed, shown in fig. 6(a), was composed of a drilling rig, a vacuum system, and an FBG measuring device. A T20WN torque transducer manufactured by Hottinger Baldwin Messtechnik GmbH, which has a 50 Nm nominal torque and 0.1 Nm measurement accuracy, was used to measure the torque. The drill is AISI1045 and approximately 2 m long. The maximum diameter of the drill bit is 32 mm, and the diameter of the drill rod is 27 mm. The height of the vacuum tank is approximately 1 m, and the diameter of the vacuum tank is approximately 0.5 m. Because the diameter of the vacuum tank is considerably larger than that of the drill, the effect of the vacuum tank on the radiation of the drill can be ignored [16]. This assumption is consistent with real condition on the Moon and theoretical analysis. The FBG sensor is arranged along the interior of the drill and installed in the drill bit near the cutting tool through a hole, as shown in figs. 6(b) and (c). The optical signal demodulator and wireless transmitting device are installed on the drill and rotate with it. The optical signal demodulator is a SmartScan model manufactured by Smart Fibres, Ltd. Its wavelength measurement accuracy is 0.005 nm, which corresponds to less than 0.6 °C in our system. A PC receives data via the wireless transmitting device and then displays and stores the data.

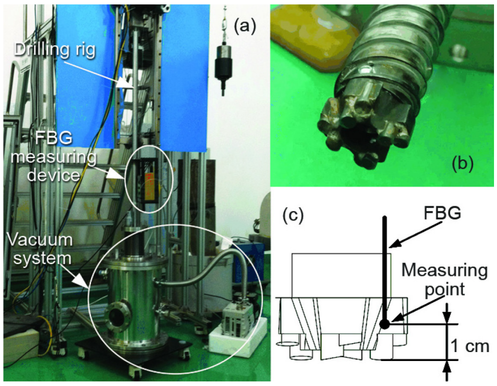

Figure 6. Experimental apparatus

It is hard to find a perfect object to simulate lunar rock. The drilling object was a loam brick, which has poor thermal conductivity and uncertain mechanical properties, similar to lunar soil and rocks. It also had good drill ability, which was convenient for observing phenomena during the experiment.

Results and discussion

Experimental results

Three experiments (Exp 1, 2, and 3) were conducted at rotational speed 108 rpm and feed rate 0.5 mm/min for 25 minutes in a vacuum of 10 Pa. The measured temperature and torque are shown in fig. 7. The temperature of drill bit is mainly affected by torque and rotational speed [17]. The curves of torque for three experiments are different from each other, resulting in the differences observed in the temperature curves. This phenomenon of torque or force variation in the same cutting conditions was also observed in cutting rock to varying degrees [18, 19]. It is believed that these variations are mainly due to the heterogeneity [20, 21] of the drilling object and partly to tool wear. So, the torque, as one input condition of the model, was difficult to control. However, it does not affect the validity of the experiments and verification for model. Further, the amount of variation observed in the experiments makes it difficult to predict the torque of the drill, which was obtained by measurement in this study.

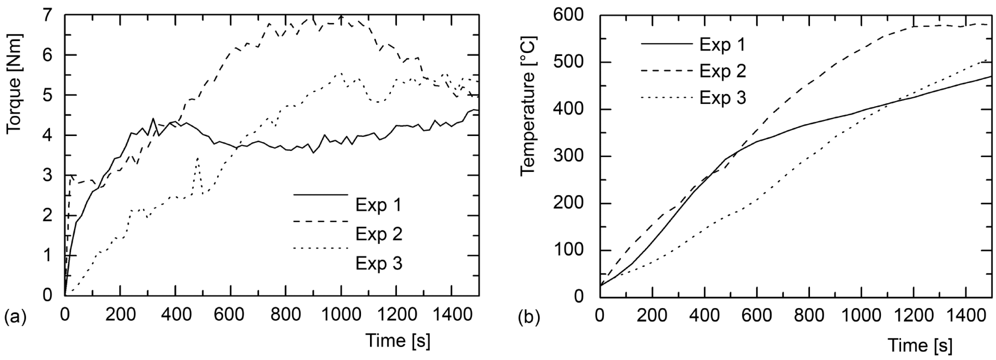

Figure 7. (a) Torque *vs.* time and (b) temperature of bit *vs.* time

Determination of correction coefficient

In this section, the correction coefficient, introduced in eq. (24), is discussed. According to the torque curves in the experiments, the power consumed during the drilling can be calculated:

$$P(\tau) = M(\tau)\omega = M(\tau)\frac{2\pi n_{\rm rot}}{180} \tag{28}$$

where $n_{\rm rot}$, rotational speed, was 108 rpm and constant in the experiments. The value was controlled by an A5 series servo motor manufactured by Panasonic, with the bias less than 2 rpm. So, it can be calculated that the power consumed has accuracy of ±3%.

The equivalent heat flow into the drill is given:

$$q_e = k_{\rm hc}k_{\rm hd}k_{\rm ms}P = k_eP \tag{29}$$

where $k_{\rm hc}$ is the coefficient of heat conversion, which is the ratio of the energy converted into heat and the total energy consumed, $k_{\rm hd}$ – the coefficient of heat distribution, which is the ratio of the heat into the drill and the total heat, and $k_{\rm ms}$ – the coefficient of model simplification, which is a coefficient that compensates for the error of simplifying the calculation model and configuration of the drill.

In this study, the three coefficients were represented by an equivalent coefficient, *i. e.*, the correction coefficient, k_e, introduced in eq. (24). It is difficult to calculate the value of k_e. However, assuming that the correction coefficient is constant for a given drill, object, and cutting environment, the value of k_e can be determined by comparing the results of finite element simulations with experimental results. Equation (29) represents thermal loads in simulations.

A model of the drill was developed in Solidworks and imported into ANSYS Workbench for thermal analysis. The modeled length of the drill was 2 m, with 1 m subject radiation conditions (note that the method for dealing with the submerged portion of the drill was the same as that described for the calculation model in the section *Impact of radiation temperature* and 1 m subject to air convection conditions. The initial temperature is 25 °C. The emissivity of drill is 0.24 and the air film coefficient is 5 W/m^{2}K. The observation point is located 1 cm from the head of the drill, which is the same location as in the experiment.

Simulations were performed with the value of the correction coefficient increasing in 0.01 increments, and the temperature at the observation point was extracted at regular time intervals. Some of the results are presented in fig. 8.

The results show that for a correction coefficient k_e value of 1, the temperature results obtained from simulation were higher than the experimental results. These results indicate that the introduction of a correction coefficient is an acceptable way to fit simulation results to experimental results and that there is a positive correlation between the temperature and the correction coefficient. The goodness of fit (D)of the simulation results to the experimental results for a given value of k_e can be expressed:

$$D = \frac{1}{n}\sum_{i=1}^{n}(T_{i2} - T_{{\rm ex}i})^2 \tag{30}$$

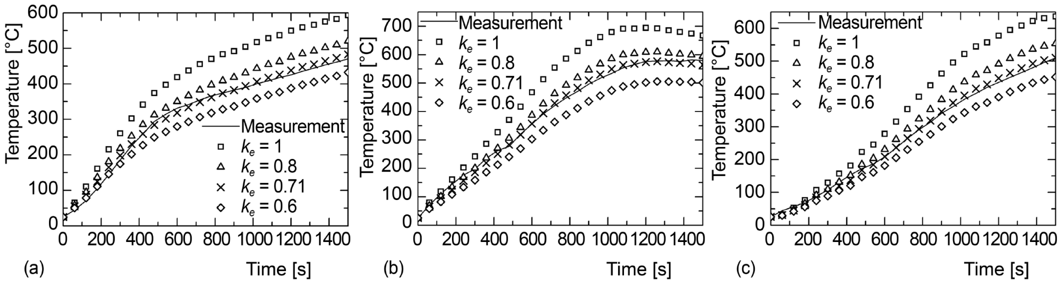

Figure 8. Comparison of simulation temperature results for various correction coefficients and experimental results for (a) Exp 1, (b) Exp 2, and (c) Exp 3

The smaller D is, the better the fit is considered to be. A comparison of the simulation results with the results of Exp 1, Exp 2, and Exp 3 shows that excellent agreement is obtained with k_e values of 0.71, 0.72, and 0.71, respectively. The mean of these three results, k_e = 0.713, was taken to be a suitable equivalent correction coefficient value for the experimental conditions considered.

Calculation results and discussion

The temperature values corresponding to k_e = 0.713 were calculated for the three sets of experimental results, and the temperature 1 cm from the head of the drill, at point x_2, was calculated. The parameter values used in the calculation are shown in tab. 1.

Table 1. Parameter values used in calculation

Parameters	Values	Parameters	Values				
r_1 [mm]	12	d_j [mm]	$j = 1$	$2 \le j \le 3$		$4 \le j \le 5$	$6 \le j \le 30$
r_2 [mm]	13.5		1.5	6		2.5	1.5
d [mm]	1.5	l	5				
A [mm^2]	120.208	x_{bj} [mm]	$j = 1$	$j = 2$	$j = 3$	$j = 4$	$j = 5$
n_{rot} [rpm]	108		2.5	6.5	15.5	16.5	26.5
τ_0 [s]	1500	A_{bj} [mm^2]	$j = 1$	$j = 2$	$j = 3$	$j = 4$	$j = 5$
$\Delta\tau$ [s]	50		76.300	240.088	424.538	373.840	192.523
$\Delta^2\tau$ [s]	1	T_0 [°C]	25				
n	30	ρ [kgm^{-3}]	$7.85 \cdot 10^3$				
n_2	50	λ [Wm^{-1}K^{-1}]	44.19				
Δx [mm]	5	c [Jkg^{-1}K^{-1}]	544				
m	30	ε	0.24				

The calculation results agree quite well with the experimental results, as shown in fig. 9. The calculations were all conducted using an ordinary dual-core PC. The time required for every set of calculations was less than 1 second. This paper does not address quantitative research on the computational time required for the calculations.

Figure 10 shows the calculated temperatures along the first 150 mm of the drill from the drill head at a time of 1500 seconds. These temperatures were calculated based on eq. (16)

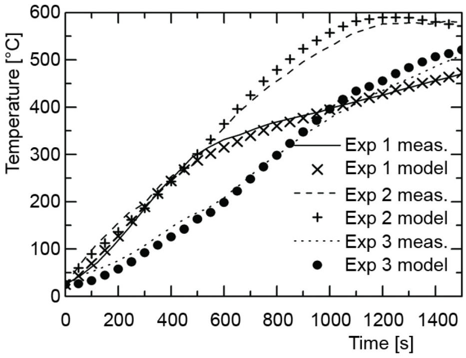

Figure 9. Comparison of calculated temperature to experimental results

according to the process shown in fig. 5 (i = 30), using the parameter values shown in tab. 1. The temperature is high near the head of the drill and decreases with increasing distance from the head. At x = 150 mm, the temperature drops to approximately 100 °C. The total radiation heat losses along the drill for the time period considered (1500 seconds) can be calculated by:

$$Q_\mathrm{r} = \sum_{i=1}^{n} c\rho d_j T_{\mathrm{r}ij} \tag{31}$$

and are shown in fig. 11. Except for the submerged part of the drill, the pattern of the total radiation heat losses is similar to that of the temperature, which is to be expected because the radiation heat loss is closely related to the temperature. The relative positions of the three curves in fig. 10 are different from those in fig. 11. This is because the total radiation heat losses depend on the temperature change over the time period from 0 to 1500 seconds, rather than the temperature at a time of 1500 seconds. Figure 11 shows that radiation has a significant impact on the temperature of the drill at high temperatures. However, the impact is slight at distances beyond x = 120 mm, where the temperature is less than 150 °C. These results suggest that sufficient accuracy can be achieved by calculating temperatures for locations along the drill where the temperature is at least 150 °C. If the temperature of the drill is high, the number or the length of the drill elements should be increased.

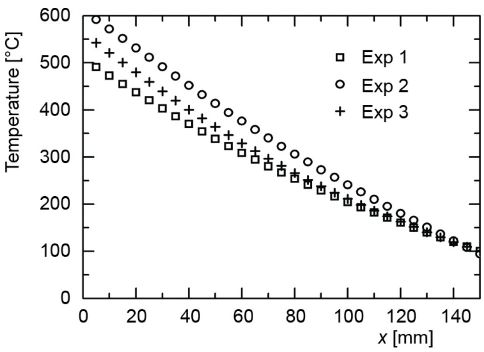

Figure 10. Calculated temperature along the drill at 1500 seconds

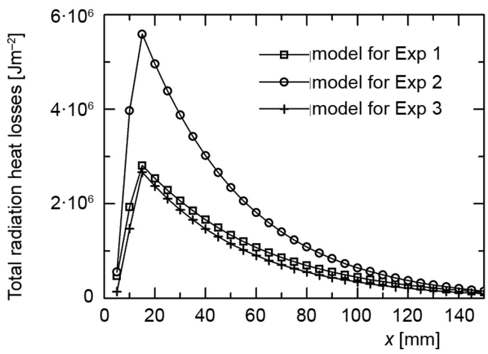

Figure 11. Total radiation heat losses along the drill over 1500 seconds

Conclusions

The temperature of a sampling drill in drilling lunar rock in a high-vacuum environment is a key concern for researchers. Based on 1-D transient heat transfer in a semi-infinite object, a fast numerical calculation method is proposed to predict the temperature of the sampling drill.

The model considered the effects of radiation, drill bit configuration, and a non-constant heat source. Radiation can be calculated only for a certain distance from the drill head. By non-uniform discretization of drill bit, the effects of different drill bit configurations on the temperature of the drill can be considered easily based on the 1-D transient heat transfer model.

An equivalent correction coefficient for the heat source and error due to model simplification is proposed in this paper. A thermal analysis was conducted using ANSYS Workbench to determine the value of the coefficient. If the value of the equivalent correction coefficient can be determined by theory rather than experiment and simulation, the analysis method will be easier and more efficient to conduct.

Because of the analytical solution of heat conduction caused by the heat source, the time step can be set to a larger value. Meanwhile, all of the time-consuming integral terms can be calculated in advance and deemed to be constants in the calculation. So, the time required for every set of calculations described in the previous section was less than 1 second on an ordinary dual-core PC.

Drilling experiments on a lunar rock stimulant were conducted in a vacuum environment using a vacuum drilling system combined with an FBG measuring device. The calculation results and the experimental results showed very good agreement.

Acknowledgment

This work was financially supported by the National Nature Science Foundation of China (No. 51105092, 61403106), the 111 Project (No. B07018), and the International Science and Technology Cooperation Program of China (No. 2014DFR50250).

Nomenclature

A – cross-sectional area, [m^2]
a – thermal diffusivity, [m^{2}s^{-1}]
C_0 – integration constant, [–]
c – specific heat, [Jkg^{-1}K^{-1}]
d – thickness, [m]
h – drilling depth, [m]
k_A – ratio of cross-sectional area of bit to rod, [–]
k_{b} – coefficient for drill bit configuration, [–]
k_e – equivalent correction coefficient, [–]
l – number of drill bit elements, [–]
M – torque, [Nm]
m – number of drill elements, [–]
n – number of time steps, [–]
n_2 – number of time elements, [–]
n_{rot} – rotational speed, [rpm]
P – drilling power, [W]
Q – energy of transient heat source, [J]
Q_{r} – total radiation heat losses, [Jm^{-2}]
q – rate of heat generation, [W]
r – average radius, $(r_1+r_2)/2$, [m]
r_1 – inner radius, [m]
r_2 – outer radius, [m]
T – temperature, [°C]
T_0 – Initial temperature, [°C]
T_{ca} – analytical expression of temperature, [°C]
V – volume, [m^3]
x, y – axial co-ordinates, [m]
Δ_x – length of drill element, [m]

Greek symbols

ε – emissivity
λ – thermal conductivity, [Wm^{-1}K^{-1}]
ρ – density, [kgm^{-3}]
σ – Stefan-Boltzmann constant, [Wm^{-2}K^{-4}]
τ – time, [s]
τ_0 – total calculating time, [s]
$\Delta\tau$ – time step, [s]
$\Delta^2\tau$ – time element, [s]
ω – rotational speed, [rads^{-1}]

Subscripts

b – drill bit
c – conduction
ex – experiment
i – relative to time
j – relative to co-ordinate
k – relative to time
r – radiation
s – sum
t – transient

References

[1] Cremers, C., *et al.*, Thermal Conductivity of Fines from Apollo 11, *Proceedings*, Apollo 11 Lunar Science Conference, Houston, Tex., USA, 1970, Vol. 1, pp. 2045-2050
[2] Keihm, S., Langseth, M., Surface Brightness Temperatures at the Apollo 17 Heat Flow Site: Thermal Conductivity of the Upper 15 cm Regolith, *Proceedings*, Fourth Lunar Science Conference, Houston, Tex., USA, 1973, Vol. 1, pp. 2503-2513

[3] Devries, M. F., *et al.*, Temperature Distributions in Drilling, *Journal of Engineering for Industry, 90* (1968), 2, pp. 231-238
[4] Saxena, U. K., *et al.*, Drill Temperature Distributions by Numerical Solutions, *Journal of Engineering for Industry, 93* (1971), 4, pp. 1057-1066
[5] Watanabe, K., *et al.*, Thermal Analyses of the Drilling Process, *Bull. Japan Soc. Prec. Eng., 11* (1977), 2, pp. 71-77
[6] Agapiou, J. S., *et al.*, On the Determination of Thermal Phenomena during a Drilling Process – Part I, Analytical Models of Twist Drill Temperature Distributions, *Int. J. Mach. Tools Manuf., 30* (1990), 2, pp. 203-215
[7] Agapiou, J. S., Stephenson, D. A., Analytical and Experimental Studies of Drill Temperatures, *Journal of Manufacturing Science and Engineering, 116* (1994), 1, pp. 54-60
[8] Fuh, K. H., *et al.*, Temperature Rise in Twist Drills with a Finite Element Approach, *International Communications in Heat and Mass Transfer, 21* (1994), 3, pp. 345-58
[9] Bono, M., Ni, J., A Method for Measuring the Temperature Distribution along the Cutting Edges of a Drill, *Journal of Manufacturing Science and Engineering, 124* (2002), 4, pp. 921-923
[10] Bono, M., Ni, J., The Location of the Maximum Temperature on the Cutting Edges of a Drill, *International Journal of Machine Tools & Manufacture, 46* (2006), 7, pp. 901-907
[11] Li, R., Shih, A. J., Tool Temperature in Titanium Drilling, *Journal of Manufacturing Science and Engineering, 129* (2007), 4, pp. 740-749
[12] Wu, J., Han, R. D., A New Approach to Predicting the Maximum Temperature in Dry Drilling Based on a Finite Element Model, *Journal of Manufacturing Processes,11* (2009), 1, pp. 19-30
[13] De Sousa, P., *et al*, Estimation of Heat Flux and Temperature Field during Drilling Process Using Dynamic Observers Based on Green's Function, *Applied Thermal Engineering, 48* (2012), 15, pp. 144-154
[14] Nedić, B. P., *et al.*, Cutting Temperature Measurement and Material Machinability, *Thermal Science, 18* (2014), Suppl. 1, pp. S259-S268
[15] Hou, X. Y., *et al.*, Thermal Test of Lunar Rock Drill Bit in Vacuum Environment, *Applied Mechanics and Material, 475-476* (2014), pp. 38-44
[16] Holman, J. P., *Heat Transfer,* 8th ed., McGraw-Hill, New York, USA, 1997
[17] Cui, J. S., *et al.*, Experimental Research on Temperature Rise of Bit in Drilling Normal and Low Temperature Lunar Soil Simulant, *Applied Mechanics and Materials, 373-375* (2013), Avg., pp. 2008-2014
[18] Nishimatsu, Y., The Mechanics of Rock Cutting, *International Journal of Rock Mechanics and Mining Sciences, 9* (1972), 2, pp. 261-270
[19] Franca, L., A Bit-Rock Interaction Model for Rotary-Percussive Drilling, *International Journal of Rock Mechanics and Mining Sciences, 48* (2011), 5, pp. 827-835
[20] Liu, H. Y., *et al.*, Numerical Simulation of the Fracture Process in Cutting Heterogeneous Brittle Material, *Int. J. Numer. Anal. Methods Geomech., 26* (2002), 13, pp. 1253-1278
[21] Villeneuve, M. C., *et al.*, Effects of Grain Scale Heterogeneity on Rock Strength and the Chipping Process, *International Journal of Geomechanics, 12* (2012), 6, pp. 632-647

Paper submitted: October 23, 2014
Paper revised: April 15, 2015
Paper accepted: April 15, 2015